



Intelligent Control Methodology for Smart Highway Bridge Structures Using Optimal Replicator Dynamic Controller

Z. Momeni ^{1*}, A. Bagchi ¹

¹Department of Building, Civil and Environmental Engineering, Concordia University, Montréal, QC H3G 1M8, Canada.

Received 02 October 2022; Revised 25 November 2022; Accepted 12 December 2022; Published 01 January 2023

Abstract

Control algorithms are an essential part of effective semi-active vibration control systems used for the protection of large structures under dynamic loading. Adaptive control algorithms, which are data-driven methods, have recently been developed to replace model-based control algorithms, thus improving efficiency. The dynamic parameters of semi-actively controlled infrastructures will change after significant vibration loading. As a result, these structures require real-time, effective control actions in response to changing conditions, which classical controllers are unable to provide. To improve the efficiency of the semi-active controller, the optimal control algorithm was developed in this study. The algorithm is the integration of the replicator dynamics with an improved non-dominated sorting genetic algorithm (NSGA), which is NSGA-II. The optimal parameters of replicator dynamics (total resources, growth rate, and fitness function), which represent the behavior of the actuators, were obtained through a multi-objective optimization process. The new control system was then used to reduce the vibrations of the isolated highway bridge, which is equipped with semi-active control devices known as MR dampers. Moreover, the current study improved the performance of the structural control system with minimum energy consumption by assigning a specific growth rate to each control device. In order to reduce the vibrations of the highway bridge, the results show that the performance of the optimal replicator controller is better than the performance of the classical control algorithms.

Keywords: Replicator Dynamics; Game Theory; Data-Driven Control; Optimization; Optimal Control; Smart Structure.

1. Introduction

Bridges are lifeline structures that support the transport of people as well as the local economy. However, the resulting damage from earthquake activities shows that bridges are vulnerable to severe earthquakes [1-3]. Injuries, loss of life, and investment are some of the consequences of bridge failure. Comprehensive studies on the financial consequences of damage to bridges caused by seismic vibrations have emphasized the importance of bridge vibration reduction strategies [4]. Conventional approaches to bridge structural design focus on clearly defined pier columns with the capacity and ductility to withstand the load. However, recently, seismic reduction seems to be the preferred solution in the design of bridges since the structure remains elastic with less damage [5]. Passive, active, and semi-active are different seismic reduction methods. Over the last two decades, passive control systems have been considered acceptable by researchers as vibration reduction systems for civil structures due to their reliability. However, passive systems are not controllable and cannot adapt to the changes that happen to the structures [6-10]. As a result, smart systems have been suggested in response to the shortcomings of passive vibration control systems to adjust dynamic structural properties such as mass and stiffness [11-15]. Smart systems are developed by using sensors, actuators, signal processors, and power sources. All in all, active and semi-active control systems are intelligently controlled systems that use actuators to gradually adjust stiffness and damping [16].

* Corresponding author: zahra.momeni24@yahoo.com

 <http://dx.doi.org/10.28991/CEJ-2023-09-01-01>



© 2023 by the authors. Licensee C.E.J, Tehran, Iran. This article is an open access article distributed under the terms and conditions of the Creative Commons Attribution (CC-BY) license (<http://creativecommons.org/licenses/by/4.0/>).

The control algorithm is an essential part of vibration control systems [17–19]. However, most of the studies in the field of vibration control emphasize control devices rather than control algorithms. An efficient control algorithm contributes to the development of a more reliable and effective control system. In order to control structural vibration, some control algorithms use mathematical models of the structure, known as "model-based controllers". An accurate numerical model of the existing structure is essential for model-based control schemes. The performance and robustness of the controller rely upon "the precise values of the dynamic parameters" of the structure [4]. However, the estimation errors in determining the dynamic parameters of the structure and simulation model result in model uncertainty. Additionally, the structure's dynamic properties may alter over time, necessitating particular considerations for ongoing model updates. Since civil structures are complex and simulating the actual behavior of the structure is challenging, there is a need for model-free, data-driven adaptive controllers that make their control decisions based on measured data, such as those derived from artificial intelligence and game theory [4, 16].

Replicator dynamics controllers belong to evolutionary game theory. It can be used to solve engineering-related resource allocation problems [4, 20]. Recently, researchers used replicator dynamic for the vibration control. Soto & Adeli investigated the replicator dynamic controller to control the building [21-24] and bridge [4, 25] structures. They proved that the performance of the replicator dynamic in vibration reduction of the building is better than the classical linear algorithms. They tried to optimally design the replicator controller to reduce the response of the structures as minimally as possible. However, the performance of the replicator controller for vibration reduction of the bridges is under investigation. Ramezani et al. [26] studied the performance of the semi-active TMD for the vibration reduction of the building considering the uncertainty. Fuzzy controller was used in their study. Bathaei & Zahrai [27] studied the performance of the MR damper in vibration reduction of the 11-story structure under seismic load. They used fuzzy controller in two different decision states. Based on the literature review, a new design of replicator dynamic integrated with optimization algorithm to determine the optimal values of the replicator dynamic parameters shows a great potential in the future of effective active and semi-active vibration control system design. In this study, replicator dynamic controller was incorporated with a multi-objective optimization algorithm known as NSGA-II to find the best values for the parameters of the controller. Moreover, this development has the advantage of using less energy in the system. The performance of the controller was improved by establishing the optimal growth rates for each control device.

The best values for the replicator dynamics parameters are determined by solving a multi-objective Pareto-based optimization problem. A multi-objectives problem has several objectives that are generally in conflict, preventing simultaneous optimization of each main objective [28]. A multi-objective optimization problem considers multiple conflicting goals at the same time. In most cases, there are multiple solutions with varying trade-offs, referred to as Pareto optimal or non-dominated solutions [29]. Despite the fact that there are multiple Pareto optimal solutions, only one is frequently chosen. Multi-objective optimization, in contrast to single-objective optimization, consists of at least two key tasks: an optimization task for discovering Pareto optimal solutions (via a computer-based procedure) and a decision-making activity for selecting the single most preferred alternative [30].

In the 1960s, a number of researchers separately argued that optimization should be based on natural evolutionary principles, particularly Darwin's theory of survival of the fittest. One feature that distinguishes these so-called evolutionary algorithms is the use of a population of solutions. This is especially useful for multi-objective optimization since it allows for the simultaneous search for many Pareto optimal solutions, giving the user a variety of options to choose from. The non-dominated sorting genetic algorithm (NSGA) introduced in [31] was one of the first EAs. NSGA-II is an improved version of NSGA that was used in this study. The NSGA-II algorithm was described in detail by Deb [32].

The objective of this research is to create a new design of replicator dynamic controller by incorporating replicator dynamic algorithm with an improved version of non-dominated sorting genetic algorithm (NSGA-II). The algorithm is used to determine Pareto optimal values for replicator dynamic parameters with the goal of improving the accuracy of the control system and decreasing the amount of energy used by the system. In addition, an intelligent control model based on game theory concept of replicator dynamics is developed for vibration control of real-world highway bridge structures subjected to earthquake loadings that are isolated from the ground and equipped with semi-active control devices. Unlike previous studies that researchers used one growth rate value for all damper devices, the idea of vibration control advanced in this study by assigning the specific growth rate to each control device. The proposed methodology is evaluated by applying it to a benchmark example based on the real bridge in southern California that has been subjected to seismic loading. The results show the performance of the optimal adaptive controller is better than classical controller.

2. Methodology

2.1. Equations of Motion

The equations of dynamic equilibrium for the nonlinear evaluation of isolated bridge equipped with semi-active MR dampers is expressed as follows [4]:

$$M\ddot{u} + C\dot{u} + Ku = -M\vartheta\ddot{u}_g + Rr + Ww \quad (1)$$

where M , C and K matrices stand for the mass, damping and stiffness of the highway structure. ϑ is the influence vector of the ground acceleration acts on the bridge; \ddot{u} , \dot{u} , u , are the floor acceleration, velocity and displacement matrices, respectively, relative to the base; \ddot{u}_g is the absolute ground acceleration. R and W are the influence matrices for the control forces, and r and w are vectors containing the forces mobilized in the passive and active control devices, respectively. Equation 1 can be formulated in state space as presented in Equation 2:

$$\dot{x} = \begin{bmatrix} \dot{u} \\ u \end{bmatrix} = Ax + B_r z_r + B_w z_w + E\ddot{u}_g \quad (2)$$

$$y = Tx + Dz + L_g \ddot{u}_g \quad (3)$$

where x refers to the state variable vector, B_r , B_w , are the mapping matrices corresponding to z_r , z_w . y is an output vector, T stands for the output matrix, D is the matrix that affects the control force vector, and L_g is the ground acceleration feed forward vector. The state-space matrices are formulated as [4, 25]:

$$A = \begin{bmatrix} [0] & [I] \\ -M^{-1}K & -M^{-1}C \end{bmatrix} \quad (4)$$

$$B_r = \begin{bmatrix} [0] \\ M^{-1}R \end{bmatrix} \quad (5)$$

$$B_w = \begin{bmatrix} [0] \\ M^{-1}W \end{bmatrix} \quad (6)$$

$$E = \begin{bmatrix} [0] \\ \vartheta\{1\} \end{bmatrix} \quad (7)$$

$$z_r = \begin{bmatrix} [0] \\ r \end{bmatrix} \quad (7)$$

$$z_w = \begin{bmatrix} [0] \\ w \end{bmatrix} \quad (9)$$

2.2. Replicator Dynamics Controller

Recently, the control community has become more interested in studying extensive distributed systems. Some of the major issues for these systems have been addressed through various methods. The challenges include large amounts of required data for efficient system functioning, the required budget associated with the required communication system, and the significant computational burden of solving for control inputs for extensive systems. One solution is to use a multiagent systems scheme, which can be expressed in game-theoretic terms [31]. Game Theory (GT) was developed by Neumann and Morgenstern using mathematics to examine human behavior and strategic decisions-making; Nash then refined and expanded GT with the introduction of the Nash Equilibrium (NE) [24]. The NE is regarded as GT's central concept. Smith improved on the NE concept and defined the Evolutionary Stable Strategy (ESS). GT in biological evolution, known as EGT, is launched by modifying the concept of the survival of the fittest, which measures an individual's ability to reproduce the next generation. For example, people who are physically fit will have a larger population in the next generation. Taylor & Jonker [16] proposed the concept of "Replicator Dynamics (RD)" to study ESS. Replicator dynamics is a concept from evolutionary game theory. In EGT, total resources are spread to the N various zones. The distribution of resources, $z_i(t)$, to those zones i , is governed by how the zones' fitness function, $f_i[t, x_i(t)]$, compares with the weighted average of all zones' fitness functions, $\varphi[t, x(t)]$. Moreover, the rate in which the resources are distributed among zones is known as the growth rate, β_i . This replicator dynamics is formally represented in this study as [22, 25]:

$$\dot{z}_i(t) = \beta_i z_i(t) \{f_i[t, x_i(t)] - \varphi[t, z(t), x(t)]\} \quad \text{for } i = 1, \dots, N \quad (10)$$

This theory could be used to develop models for resolving resource allocation problem in engineering. To solve this type of problem, a limited resource (voltages of MR damper devices in this study) need to be assigned to multiple consumers in order to attain a given objective. Each consumer is given a fitness function that describes its ability to receive voltage. The fitness values of different consumers are then compared, and those with more fitness are given higher voltage [4, 24]. Replicator dynamics is a resource allocation problem-solving methodology. A new design for developing optimal replicator dynamic is conducted in this study to reduce the structural response of a smart highway bridge under seismic load. To accomplish this, the control devices, installed on the bridge (hereafter the MR dampers) assume the role of consumers, and the total available electrical voltage, P , is allocated to the dampers [25].

$$P = \sum_{i=1}^N z_i(t) \quad (11)$$

where N represents the total number of MR dampers. The distribution of voltage among control devices is decided by how the fitness function of each device relates to the weighted average fitness function of all devices, φ . The objective may be to achieve the smallest or highest reward. Given the available resources, the former is used in vibration reduction

problem to achieve the least displacement/velocity/acceleration [24]. The value of the fitness function is derived based on positive and negative sensor measurements of the structure. In population dynamics, however, the fitness function must be strictly positive. Therefore, it is advised two replicator controllers to use. The fitness function employed for each actuator in this study is determined as follows [25]:

$$f_i^{(1)}[t, x_i(t)] = \max_t[x_i(t), 0] \quad x_i > 0 \quad \text{for } i = 1, \dots, N \quad (12)$$

$$f_i^{(2)}[t, x_i(t)] = \max_t[-x_i(t), 0] \quad x_i < 0 \quad \text{for } i = 1, \dots, N \quad (13)$$

The fitness function is therefore purely positive and is calculated with the present structural sensor data considered. It produces the voltage necessary for the i^{th} actuator to achieve the control aim, such as minimizing displacement or the total voltage of the control devices. To make the control system economical, the power is limited by adding a fictitious control device, z_{N+1} [24]. The weighted average fitnesses $\varphi^{(1)}$ and $\varphi^{(2)}$ are represented as follows [21]:

$$\varphi^{(1)}[t, x(t), z(t)] = \frac{1}{p} \sum_{i=1}^{N+1} z_i^{(1)} f_i^{(1)}[t, x_i(t)] \quad (14)$$

$$\varphi^{(2)}[t, x(t), z(t)] = \frac{1}{p} \sum_{i=1}^{N+1} z_i^{(2)} f_i^{(2)}[t, x_i(t)] \quad (15)$$

f_{n+1} is the fictitious fitness function, and it is adjusted to relatively small positive number to collect voltage when the structure does have substantial displacement [33]. Now, using the following replicator equation, the ultimate voltage of each MR damper can be determined as follow:

$$z_i(t) = [z_i^{(2)}(t) - z_i^{(1)}(t)] \quad i = 1, \dots, N \quad (16)$$

There are two replicator controllers. One is utilized to determine the positive state, while the other determines the negative state. When the displacement measurement at a certain time, t , is positive, the voltage from the first replication will be positive and the voltage from the other replicator will be zero. When the difference between the positive and negative replicators is negative, the actuator's voltage will be negative as well. This indicates that the voltage is delivered in opposition to the motion [24].

2.3. Multi-Objective Optimization of Replicator Control Parameters Using NSGA-II

Recently, multi-objective optimization has been proposed for addressing engineering application. Multi-objective optimization refers to the process of optimizing systematically and simultaneously multiple objective functions [33]. Generally, the primary goals for many-objective problems are in conflict, and simultaneous optimization of the goals is not possible. Multiple goals are common in many practical engineering problems, such as optimizing performance and reliability while lowering expense [20, 34]. Bridge control problems related to many influencing factors, including the main objectives, optimization variables, and constraints, lead to being best solved with multi-objective algorithms. Several objectives in a problem give rise to a set of optimum solutions (often known as Pareto-optimal solutions) rather than a single optimal solution. Without further information, it is impossible to identify which of these Pareto-optimal solutions is superior. This necessitates that the user discovers as many Pareto-optimal solutions as possible [33].

The general problem of multi-objective optimization is stated as follows:

$$\min_x F(x) = [F_1(x), F_2(x), \dots, F_k(x)]^T \quad (17)$$

$$\text{Subject to } g_j(x) \leq 0, \quad j = 1, 2, \dots, n \quad (18)$$

$$h_l(x) = 0, \quad l = 1, 2, \dots, e \quad (19)$$

where k , n , and e are the number of objective functions, inequality constraints, and equality constraints, respectively. $g_j(x)$ is the j^{th} inequality constraint function, $h_l(x)$ is the l^{th} equality constraint function [34, 35].

2.3.1. The Fast and Elitist Multi-Objective Genetic Algorithm NSGA-II

From 1993 to 1995, a variety of evolutionary algorithms were offered for solving multi-objective optimization problems. More attention was paid to Fonseca and Fleming's MOGA, Srinivas & Deb's NSGA, and Horn et al. NPGA's [28]. NSGA-II is among the most well-known multi-objective optimization algorithms with three distinctive features: a fast-non-dominated sorting approach, a fast-crowded distance estimation method, and a simple crowded comparison operator. Deb et al. [32] recreated several experiments from a previous study utilizing the NSGA-II optimization technique, and it is declared that this approach outperformed other evolutionary optimization algorithms in terms of discovering a wide and varied range of answers [36]. NSGA-II can be roughly described as the following steps including Initialization of the population, non-dominant sorting, assigning crowding distance, multiple recombination and selection.

2.3.2. Multi-Objective Structural Control Problem

The efficiency of the controller utilizing replicator dynamics depends on 3 key parameters including the total population (total sum of actuator voltage for control), P , the growth rate, β , and the value of the fictitious floor fitness function, f_{N+1} . The replicator controller is combined with a multi-objective optimization algorithm to determine Pareto optimal values for P , f_{N+1} and growth rates β_i ($i = 1$ to N where N is the total number of devices) aiming to maximize the structural performance while reducing power consumption. In the previous attempts of researcher for the vibration reduction of highway bridge, one growth rate was determined for the control system. However, in this study the idea has been improved. Therefore, each control device has its own growth rate, the value of which is determined by a multi-objective optimization procedure. Based on the replicator dynamics described in detail in the preceding sections, the replicator's fitness functions play a crucial role in the resource allocation problem and, in this study, it is determined based on the sensor measurements. The objectives of the methodology developed in this study are minimizing the several criteria defined in the Table 1.

Table 1. Definition of performance criteria used as the objectives of the vibration control problem [25]

Performance Criteria	Definition	formula
J_1	Maximum shear in controlled state divided by maximum uncontrolled shear response.	$J_1 = \max_t \frac{ V_b(t) }{V_{b,max}}$
J_2	Peak overturning moment in controlled state divided by maximum uncontrolled overturning moment.	$J_2 = \max_t \frac{ M_b(t) }{M_{b,max}}$
J_3	Maximum mid-span displacement in controlled state, divided uncontrolled mid-span displacement.	$J_3 = \max_t \frac{ u_m(t) }{u_{m,max}}$
J_4	Maximum mid-span acceleration in controlled state, divided by the uncontrolled mid-span acceleration.	$J_4 = \max_t \frac{ \ddot{u}_m(t) }{\ddot{u}_{m,max}}$
J_5	Maximum bearing deformation in controlled state, divided by maximum uncontrolled bearing deformation.	$J_5 = \max_t \frac{ u_b(t) }{u_{b,max}}$
J_6	Maximum column curvature in controlled state, divided by uncontrolled column curvature.	$J_6 = \max_t \frac{ \varphi(t) }{\varphi_{max}}$
J_9	Normed maximum shear in controlled state divided by the maximum uncontrolled shear response.	$J_9 = \max_t \frac{\ V_b(t)\ }{\ V_{b,max}\ }$
J_{10}	Normed peak overturning moment in controlled state divided by uncontrolled overturning moment.	$J_{10} = \max_t \frac{\ M_b(t)\ }{\ M_{b,max}\ }$
J_{11}	Normed mid-span displacement in controlled state, divided by uncontrolled midspan displacement.	$J_{11} = \max_t \frac{\ u_m(t)\ }{\ u_{m,max}\ }$
J_{12}	Normed mid-span acceleration in controlled state, divided by uncontrolled midspan acceleration.	$J_{12} = \max_t \frac{\ \ddot{u}_m(t)\ }{\ \ddot{u}_{m,max}\ }$
J_{13}	Normed bearing deformation in controlled state, divided by uncontrolled bearing deformation.	$J_{13} = \max_t \frac{\ u_b(t)\ }{\ u_{b,max}\ }$
J_{14}	Normed column curvature in controlled state, divided by uncontrolled column curvature.	$J_{14} = \max_t \frac{\ \varphi(t)\ }{\ \varphi_{max}\ }$
J_{15}	Peak control force in controlled state divided by the weight of the bridge structure.	$J_{15} = \max_t \frac{ z_i(t) }{W}$
J_{16}	Peak stroke of the kth control device, divided by peak deformation bearing of the uncontrolled structure.	$J_{16} = \frac{\max_t u_k(t) }{\max_t \ u_b(t)\ }$

3. Application

3.1. Description of the Bridge

To assess the proposed techniques, Nagarajaiah's benchmark control problem is used [1-3]. This problem is developed based on the real-world isolated highway bridge situated in California equipped with fluid viscous dampers subjected to seismic loading. MATLAB and SIMULINK are used to generate the mathematical model of the bridge as well as the model of the control system. "108 nodes, 430 DOF, 70 beam elements, 4 rigid links, 24 springs, 8 bearings at abutments, and 27 dashpots" [4] are part of the bridge finite element model [1]. This model is employed as the bridge's evaluation model. The frequency range of the bridge is between 1.23 (HZ) and 4.65 (HZ), which corresponds to the transverse and longitudinal frequencies of the bridge structure. Natural frequencies of the structure are presented in Table 2. 20 MR dampers are included in the bridge model at 10 distinct points to reduce the dynamic response of the bridge. Figure 1 depicts the benchmark bridge's overall configuration. The 3D perspective of the MR dampers linking

the deck to the abutments is shown in Figure 2. Figure 2 also shows how the sensors and control devices are arranged. Overall configuration of the MR dampers is shown in Figure 3. The benchmark bridge structure's modal characteristics are displayed in Table 2. Makris & Zhang [37] provide a full derivation of the dynamics of the highway bridge, whereas Agrawal et al [1] provide a complete derivation of the finite element model's transfer from ABAQUS into MATLAB computational formulation.

Table 2. Natural frequencies of the simulation model [25]

Mode Num	Natural Frequency (Hz)	Mode
1	1.25	Torsional
2	1.35	Torsional + Vertical
3	2.18	Vertical
4	2.54	Transverse
5	3.2	2 nd Vertical
6	4.65	2 nd Transverse

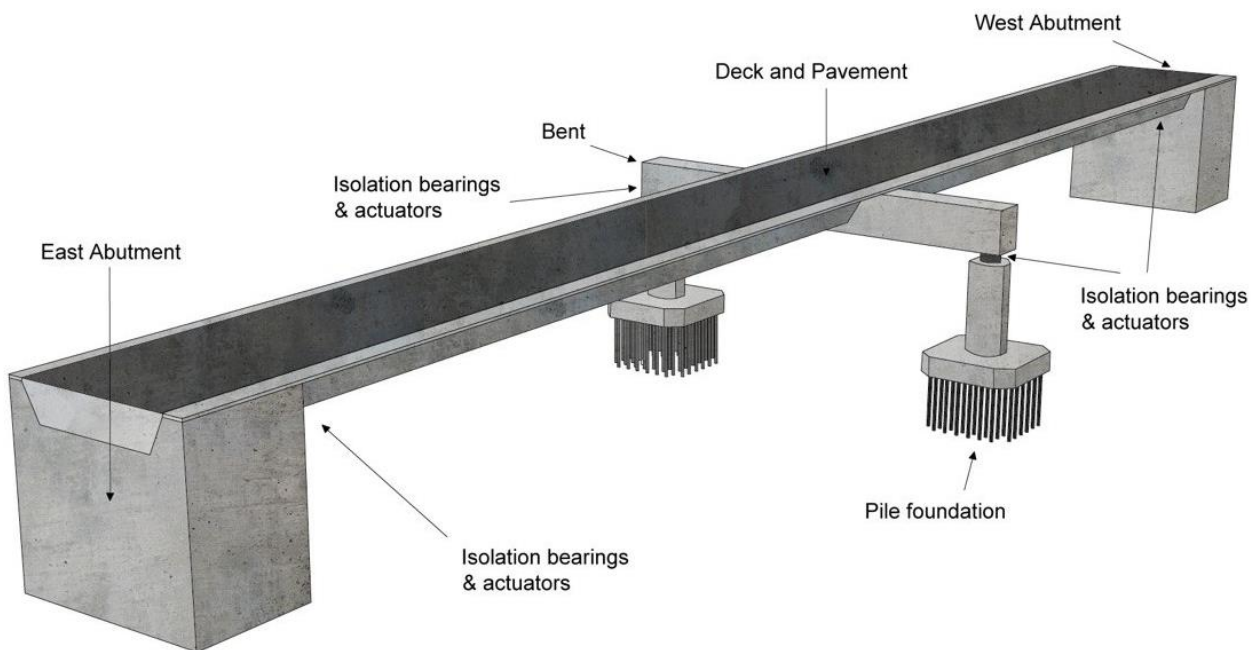


Figure 1. The 3D bridge's overall configuration [25]

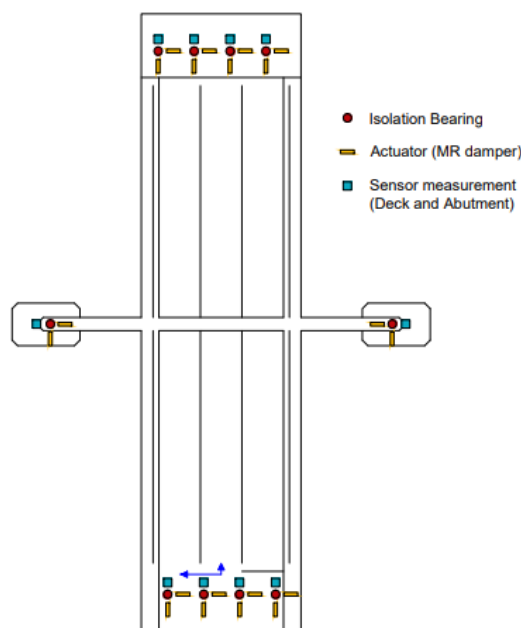


Figure 2. Arrangement of sensors and control devices [25]

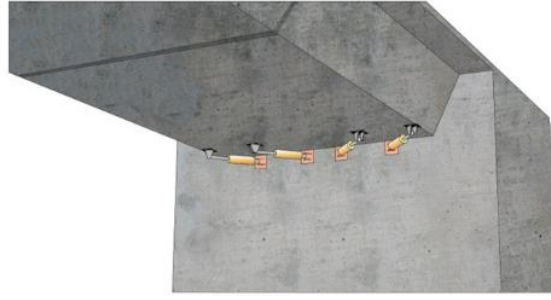


Figure 3. Overall configuration of the MR dampers [25]

3.2. MR Damper Model

Magneto-rheological (MR) fluids are oily substances containing magnetic suspended particles. In the presence of an applied magnetic field the ions align themselves along the magnetic field and turn into dipoles. The suspensions transits from a free-flowing state to a semi-solid state under magnetic field results in developing the yield stress. This phenomenon may take place in a matter of milliseconds. In order to use the specific features of MR dampers in application of controlling vibration, a numerical model that introduces the MR damper behavior precisely must be used. The mathematical model of the MR damper is based on Bouc-Wen hysteretic model in parallel with a dashpot added for a nonlinear ‘roll-off’ effect. The equations governing the force produced by this model of MR damper are given as:

$$h = \alpha w + c_0 \dot{q} \quad (20)$$

$$\dot{w} = -\gamma |\dot{q}| |w| |w|^{n-1} - \delta \dot{u} |w|^n + Q \dot{q} \quad (21)$$

where \dot{q} stands for the relative velocity of the MR device, w is the evolutionary variable. $\gamma, n, \delta,$ and Q are characteristics connected to the form of the hysteresis loop that determine the linearity in the unloading and the smoothness of the shift from the pre-yield to the post-yield area. Table 3 present the values of the mechanical properties of the MR dampers. The relationship between control voltage V_c and device parameters is described as follows:

$$\alpha = \alpha_a + \alpha_b + c_{0b} V_c \quad (22)$$

Moreover, resistance and inductance present in the circuit provide this system a dynamic characteristic. This dynamic behavior is calculated by the first-order filter applied to the control input as follows:

$$\dot{V}_c = -\mu(V_c - V_a) \quad (23)$$

where V_a represents the control circuit's command voltage and μ is the time constant of the first-order filter. The MR damper parameters shown in the Table.3 were chosen so that the device has had a 1000 kN capacity and a maximum command voltage of 10 V.

Table 3. The mechanical properties of the MR damper [25]

Parameter	Value	Parameter	Value	Parameter	Value
α_a	1.0872×105 N/cm	c_{0b}	44.0 N sec/(cm V)	δ	3 cm ⁻¹
α_b	4.9616×105 N/(cm V)	Q	1.2	γ	3 cm ⁻¹
c_{0a}	4.40 N sec/cm	n	1	μ	50 ec ⁻¹

4. Evaluation

The highway bridge is close to existing faults: the Newport Inglewood fault zone is 20 kilometers to the south-west, and the Whittier–Elsinore fault is 11.6 kilometers to the north-east. Dynamic analyses are used to determine the dynamic response of the bridge subjected to six earthquake records. Table 4 presents the properties of these earthquake records.

Table 4. Properties of selected earthquake records [1]

Recording Station	Earthquake	Magnitude	Distance to Fault (km)	Peak Acceleration (g)	Peak Velocity (cm/s)
North Palm Springs	1986 N. Palm Springs	6.0	7.3	0.492	73.3
TCU084	1999 Chichi	7.6	10.39	1.157	114.7
El Centro	1940 Imperial Valley	7.0	8.3	0.313	29.8
Rinaldi	1994 Northridge	6.7	7.1	0.838	166.1
Bolu	1999 Duzce, Turkey	7.1	17.6	0.728	56.4
Nishi-Akashi	1995 Kobe	6.9	11.1	0.509	37.3

5. Results and Discussion

Many-objectives optimization problem is solved in this study to examine the effect of replicator parameters in reduction of the dynamic response of bridge structure subjected to earthquake records. Selection of the optimal replicator dynamic parameter values is crucial to replicator dynamic performance. In the recent studies [25, 33], the author conducted a sensitivity analysis to find the best values for the replicator dynamic parameters that is time-consuming and unreliable. In this study, however, the author enhances the precision of the outcomes by combining the replicator dynamic algorithm with the multi-objective NSGA-II algorithm in order to find the optimal Pareto front of replicator dynamic parameters and use optimal replicator dynamic controller for the vibration reduction of the highway benchmark structure subjected to seismic loading. Here, two different ideas investigated and compared for the vibration reduction of the highway bridge structure. To study the influence of replicator parameters on the whole control system, the author used the idea of centralized and decentralized approaches. For the centralized approach, we use the single-agent Centralized Replicator Controller (CRC) and we determine the replicator parameters (β, P, f_{n+1}) for the system. In the next step, the effectiveness of the single-agent Centralized Replicator Controller (CRC) is compared with the decentralized Multi-Agent Replicator Controller (MARC). For the decentralized approach, we use the Multi-agent Replicator Controller (MARC) and we determine the replicator parameters $(\beta_i, \beta_{n+1}, P, f_{n+1})$ for the system. The objective is to compare the efficiency of two types of replicator controller and to determine the relation between the growth rate parameter of each replicator controllers and the structural vibration reduction performance when subjected to a variety of earthquakes. To achieve this goal, the replicator control parameters including ten different growth-rate for each MR devices plus fictitious growth rate, the total resources (total sum of the actuator voltages), P , the fictitious floor fitness function, f_{n+1} are set to be the design variables of the optimization problem, $\theta_o = [\beta_i, \beta_{n+1}, f_{n+1}, P]$. And, the design objectives for this many-objectives optimization problem are to minimize the all performance criteria (J_1 to J_{16}) simultaneously including the structural responses as well as the power consumption and actuator forces $\mathbf{J}(\theta) = [J_1(\theta) \dots J_{16}(\theta)]^T$.

The following section shows the results of the study. The higher and lower boundaries of the replicator dynamic parameters and the NSGAI parameter values are shown in Tables 5 and 6, respectively. Setting the parameter range enables the process to be sustainable, since the same performance can be obtained with fewer resources.

Table 5. Upper and lower bounds for replicator dynamic variables

P	f_{n+1}	β_i	V_i (Volt)	Variable/parameter
[5,200]	[0,10]	[0.001,20]	[-10,10]	Range

Table 6. NSGA-II parameters

Maximum iteration	Mutation Percentage	Crossover percentage	Population size	Parameter
100	0.4	0.7	50	Value

Figure 4 depicts the NSGA-II flow diagram for the semi-active control of the highway bridge structure. During the seismic loading, the iterative procedure is used to determine the optimal values for replicator dynamic parameters at each time step. The initial parameters of NSGA-II, including population size, maximum iteration procedure, and selection of crossover and mutation probability, are utilized to generate a random parent population, POP_0 , or total number of chromosomes of size N . The optimization problem's solutions are chromosomes composed of thirteen parameters: total resources, P , growth rate for each MR damper, β_i, β_{n+1} , and fictitious function, f_{n+1} .

In this study, the vector of objective functions of the optimization problem consist of 13 different objectives, including "maximum base shear (J1), overturning moment (J2), midspan displacement (J3), acceleration (J4), maximum bearing deformation (J5), maximum ductility (J6), maximum RMS of base shear (J9), maximum RMS of base moment (J10), maximum RMS of midspan displacement (J11), maximum RMS of midspan acceleration (J12), maximum RMS of abutment displacement (J13), maximum RMS of ductility (J14) and (J16) maximum stroke of control device" [33], that are minimized by optimal values of replicator dynamic parameters. Then, the crowding distance of the sorted solutions is calculated on all fronts. Tournament selection is then used to generate a new parent population of size N in order to activate the crossover and mutation operators. In the subsequent step, the aforementioned operators are applied to the newly-created parent population to generate the N -member offspring population Q_s . The values of the objective function are determined by the offspring population. Next, the parent and progeny populations are combined to form a new population of size $2N$, R_i . The non-dominated fronts and crowding distance are found and created for the new population R_i . The optimization procedure concludes if the termination condition is met. Otherwise, the preceding procedure must be repeated until the maximum number of iterations has been reached.

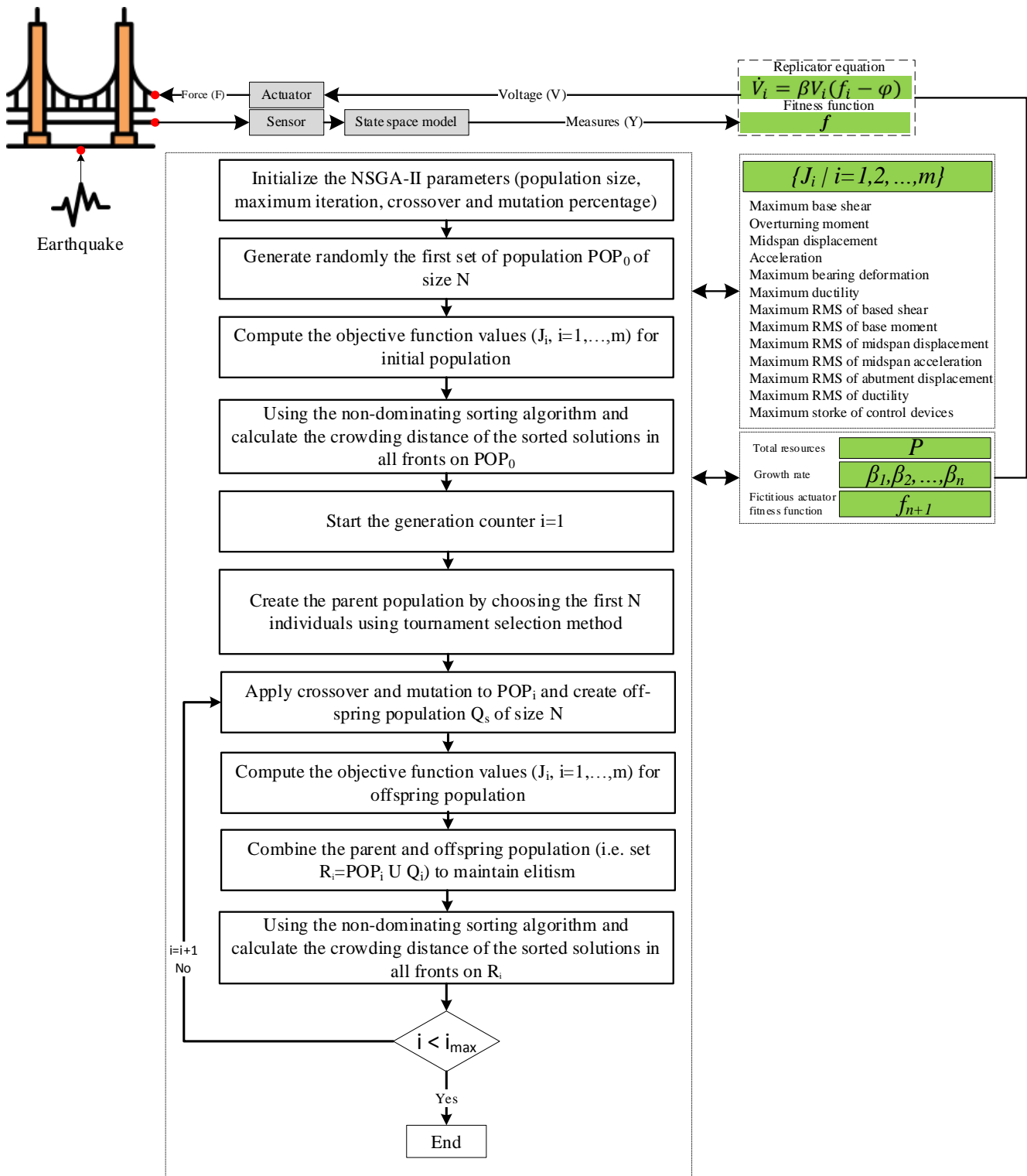
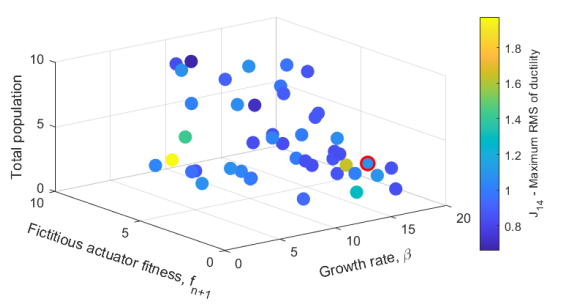
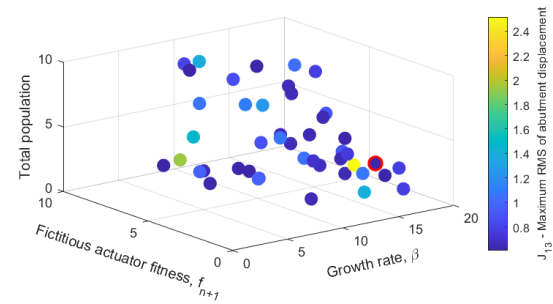
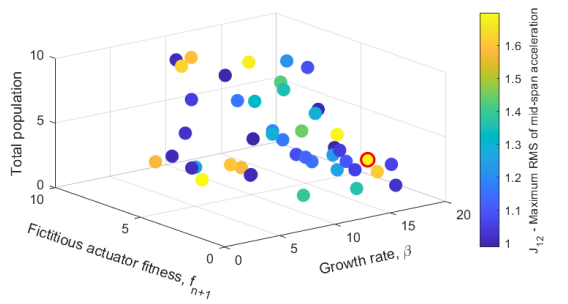
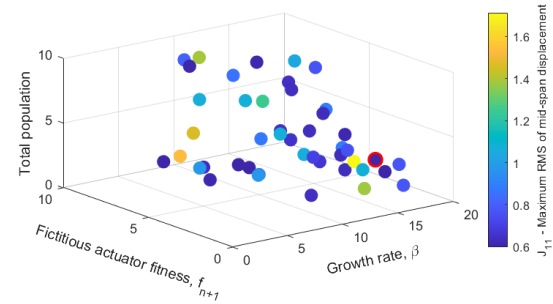
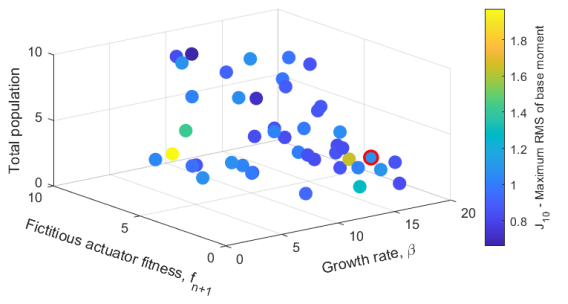
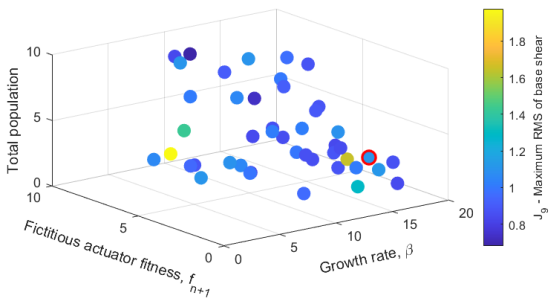
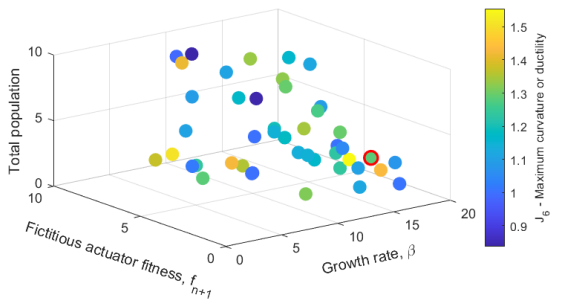
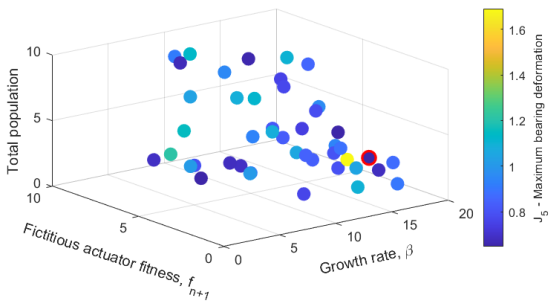
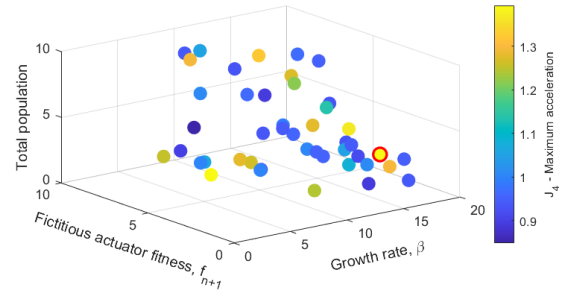
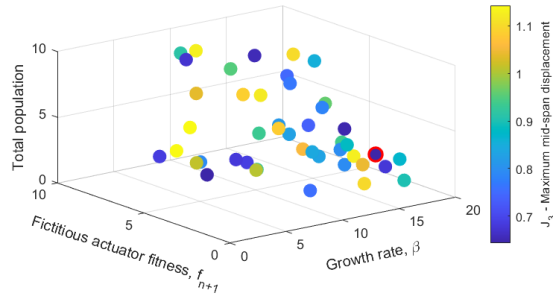
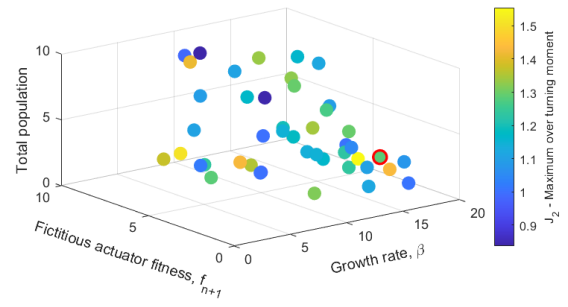
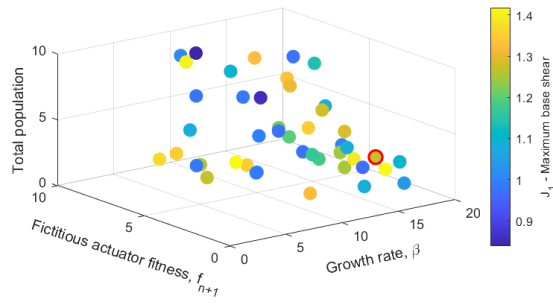


Figure 4. The NSGA-II flow diagram

The optimization model provides the Pareto optimal set of replicator dynamic parameters for each earthquake. 3D Plots presented in Figure 5 are the Pareto optimal set correspond to the design variables (Total population, growth rates, fictitious fitness function) for the decentralized Multi-Agent Replicator Controller (MARC) that shows the results of performance criteria for the Elcentro earthquake. The blue colors show smaller values of the performance criteria, indicating their better values for reducing vibration. The yellow colors show larger/worse values of the performance criteria. In each plot of the Figure 5, one of the solutions of the Pareto optimal set for design variables (replicator dynamic parameters) was marked by the red rings, as a sample. Selected point presents the appropriate results for J3, J6, J11, J13, J16 performance criteria, however it provides poor results for J4, J12 performance criteria.



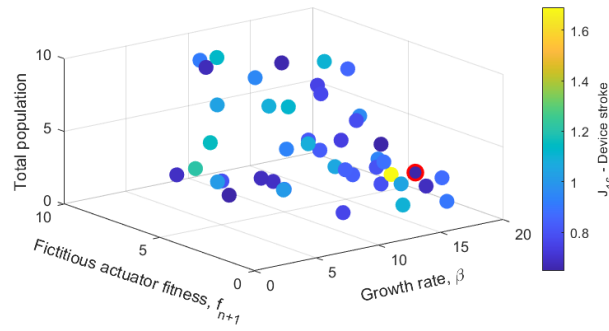
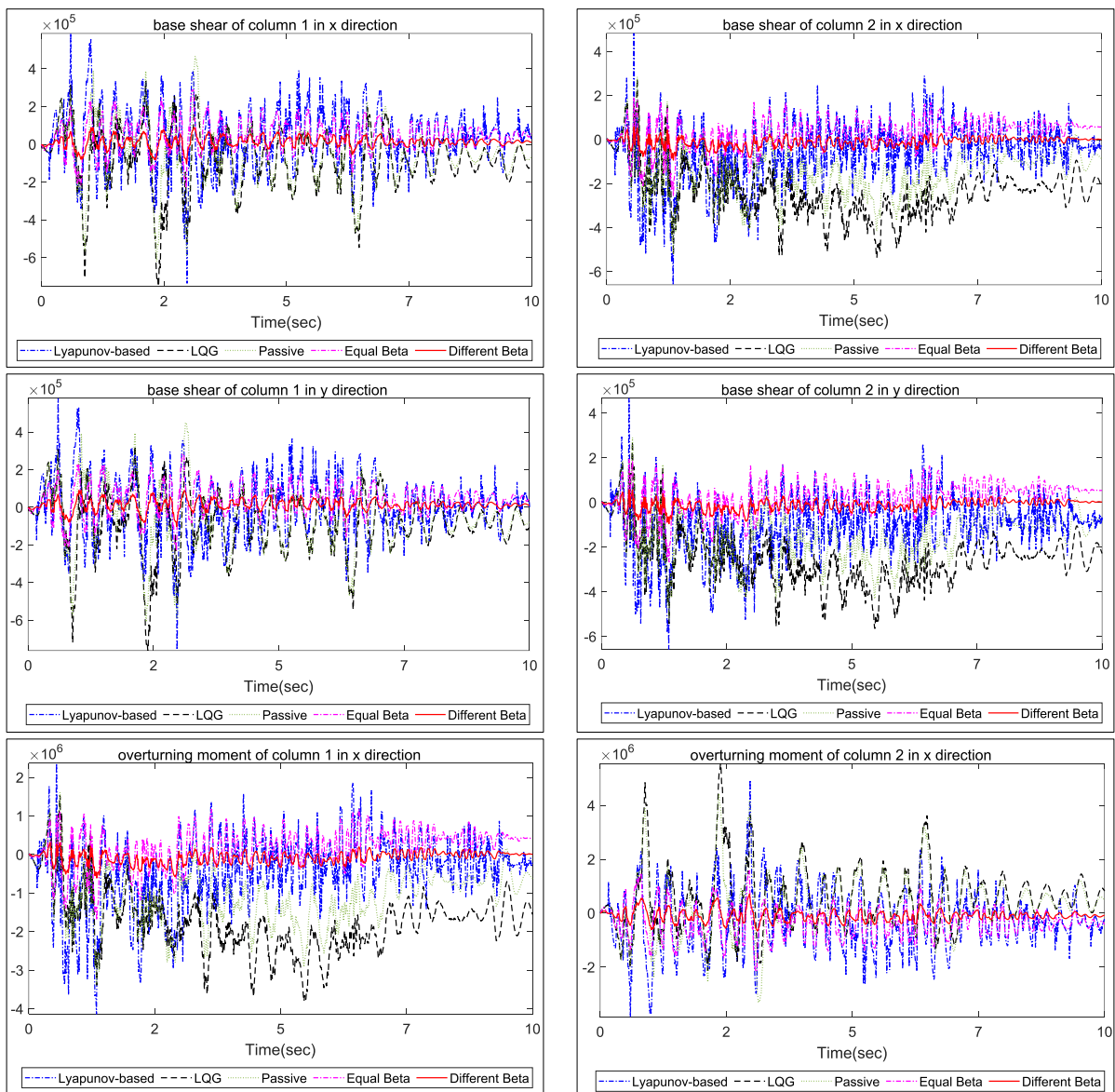


Figure 5. Performance criteria based on all Pareto solutions obtained by NSGA-II, Elcentro Earthquake

The results of this study were compared with semi-active Lyapunov, active LQG, passive systems, as well as the work of Soto and Adeli [25]. Figure 6. shows time-history results comparison of five control approaches: passive base isolation, LQG, Lyapunov-based, as well as the a single-agent Centralized Replicator Controller (CRC) and a decentralized Multi-Agent Replicator Controller (MARC) when the parameters of replicator dynamic were determined by NSGA-II and the bridge is subjected to near-fault El Centro historical earthquake. The efficiency of the proposed control algorithm is superior to LQG, passive systems, and Lyapunov-based control algorithms. However, it seems the efficiency of the single-agent Centralized Replicator Controller (CRC) is almost equal to a decentralized Multi-Agent Replicator Controller (MARC). Table 7 presents a comparison of the results obtained in this research with the passive control, semi-active Lyapunov-based control, and active LQG algorithms and the work by Soto & Adeli [25]. The superior results of the proposed algorithm were shown by the stars in Table 7.



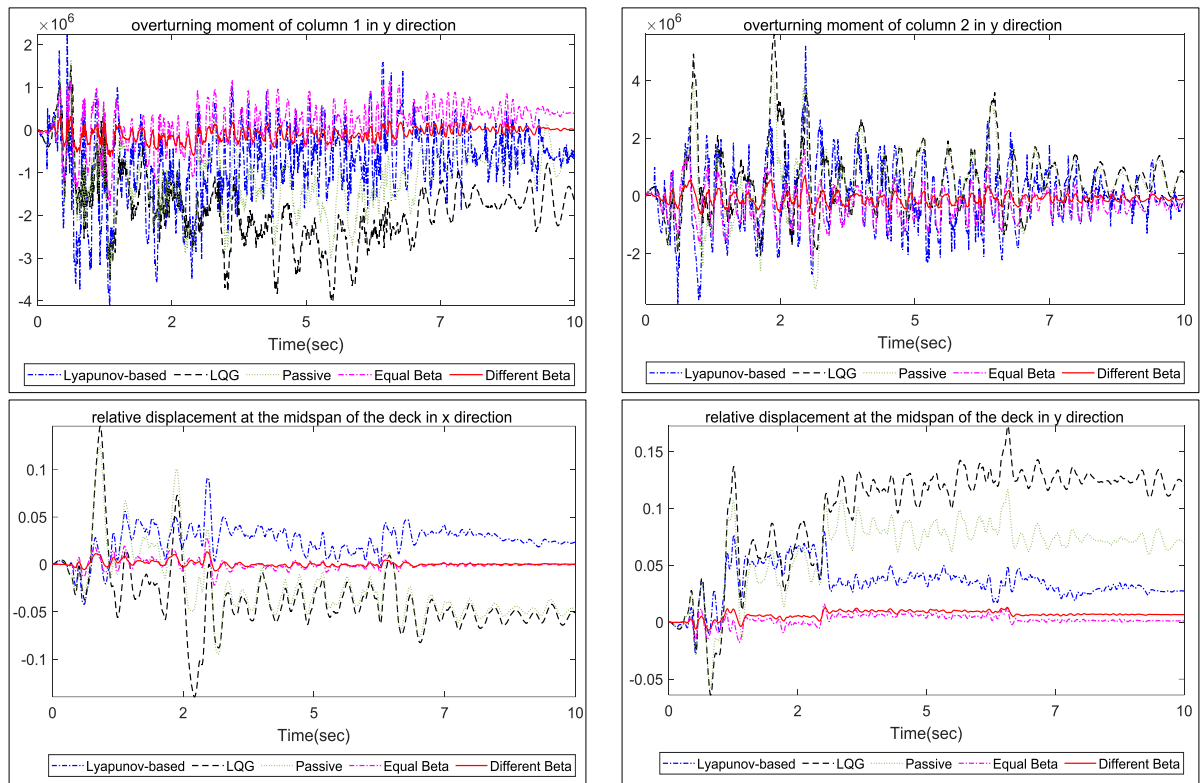


Figure 6. Comparison between controlled responses for Lyapunov, LQG, Passive control methods and the proposed method) for Elcentro earthquake

Table 7. Comparison between the results of the proposed method with competing models in each earthquake

Earthquake	Performance criteria	Benchmark			Soto & Adeli (2019) [25]	CRC	MARC	
		Passive	LQG Active	Lyapunov Semi-Active				
North Palm Spring	J1	1.057606202	0.937154735	0.919494158	0.78	0.804350559***	0.804350559***	
	J2	1.095858845	0.918512617	1.034929869	0.82	0.908223969***	0.903167643***	
	J3	0.867934706	1.010173646	0.556613594	0.8	0.756894231***	0.654856008***	
	J4	1.174329596	1.12560996	1.56643623	1.15	0.989729464***	0.989729464***	
	J5	0.884392008	1.007216871	0.563624684	0.76	0.703708739***	0.703698739***	
	J6	1.095858845	0.918512617	1.034929869	0.82	0.908223969***	0.903167643***	
	J9	1.185867268	0.968569456	0.669697967	0.96	0.755265975***	0.750287004***	
	J10	1.205091332	0.96669717	0.659772373	0.96	0.760054566***	0.754792013***	
	J11	1.015192128	0.940677911	0.430431634	0.96	0.361484191***	0.360732190***	
	J12	0.912725511	0.907865059	1.594134401	1.01	0.980439738**	0.980439737**	
	J13	1.025032368	0.941155875	0.417733692	0.91	0.337328965***	0.337125964***	
	J14	1.205091332	0.96669717	0.659772373	0.96	0.760054566***	0.754792013***	
	J16	0.884392008	1.007216871	0.563624684	0.76	0.703708739***	0.703697739***	
	Chi-chi	J1	0.909227078	1.05019981	0.915440805	0.77	0.797105552***	0.797105551***
		J2	0.946900368	0.974377337	0.886878456	0.83	0.918465136**	0.915898796**
		J3	0.761416107	1.092287607	0.741032005	0.9	0.874195258*	0.799999208**
J4		1.128194174	0.95036827	1.133848765	0.99	0.974528989***	0.964792787***	
J5		0.758203136	1.090154785	0.744439354	0.89	0.864516275**	0.804135322**	
J6		0.946900368	0.974377337	0.886878456	0.83	0.918465136**	0.915898796**	
J9		0.98468445	1.114092524	1.004966005	0.78	0.851052151***	0.790282312***	
J10		0.983743836	1.099446836	0.99637084	0.77	0.830349791***	0.764642231***	
J11		0.981185837	1.27228078	0.904406069	0.73	0.59091261***	0.590118611***	
J12		1.191318963	1.013701022	1.584488126	1.03	1.002332825***	0.982077969***	
J13		0.982214211	1.30529971	0.905981635	0.72	0.595055792***	0.593541676***	
J14		0.983743836	1.099446836	0.99637084	0.77	0.830349791***	0.764642231***	
J16		0.758203136	1.090154785	0.744439354	0.89	0.864516275**	0.804135322**	

Elcentro	J1	0.623165265	0.76528979	0.76075267	0.62	0.603900339****	0.603900339****	
	J2	0.605949578	0.766974772	0.710664526	0.63	0.579856053****	0.573249317****	
	J3	0.501855521	0.688060493	0.364672846	0.62	0.273339924****	0.273339924****	
	J4	1.094478444	0.789144506	1.352958823	1.14	0.927872419***	0.927872418***	
	J5	0.489827258	0.729033263	0.345794956	0.69	0.254361984****	0.254361984****	
	J6	0.605949578	0.766974772	0.710664526	0.63	0.579856053****	0.573249317****	
	J9	0.613150408	0.919173542	0.535234351	0.63	0.630135739**	0.62530393**	
	J10	0.604479779	0.914914136	0.512234207	0.62	0.622226367**	0.617372918**	
	J11	0.594169188	0.915780708	0.324351701	0.47	0.114224227****	0.114224227****	
	J12	0.950748703	0.896204403	1.23227818	1.03	0.988622926**	0.988622925**	
	J13	0.616556419	0.955152715	0.331357505	0.48	0.102155194****	0.102155193****	
	J14	0.604479779	0.914914136	0.512234207	0.62	0.622226367**	0.617372918**	
	J16	0.489827258	0.729033263	0.345794956	0.69	0.254361984****	0.254361984****	
	Northridge	J1	1.074776543	0.855294539	0.895672013	0.77	0.967533331*	0.83500444**
		J2	1.044544476	0.959493324	0.861585985	0.83	0.973632652*	0.834026421***
		J3	0.900390393	0.985605438	0.693980413	0.9	0.643176282****	0.643031282****
J4		1.046880633	0.927680598	1.339589936	0.99	0.826847937****	0.826847937****	
J5		0.90092364	0.986030762	0.699239607	0.89	0.647796404****	0.647302115****	
J6		1.044544476	0.959493324	0.861585985	0.83	0.973632652**	0.834026421***	
J9		0.835350194	0.794349918	0.738133628	0.78	0.842794946	0.672957688****	
J10		0.820241932	0.788120572	0.702713263	0.77	0.832295255	0.652109241****	
J11		0.759245098	0.792985182	0.456647237	0.73	0.598295964**	0.597837563***	
J12		0.976623922	0.888342111	1.241990703	1.03	0.971874609***	0.971874608***	
J13		0.763853437	0.788769388	0.464376987	0.72	0.605993903***	0.605566159***	
J14		0.820241932	0.788120572	0.702713263	0.77	0.832295255	0.652109241****	
J16		0.90092364	0.986030762	0.699239607	0.97	0.647796404****	0.647012115****	
Düzce		J1	0.778636827	0.962604251	0.826458046	0.98	0.738115585****	0.738081895****
		J2	0.704707785	0.968231091	0.868430952	0.99	0.774819744***	0.773318788***
		J3	0.591155173	0.92584006	0.363929082	0.96	0.489521415***	0.488832205***
	J4	0.916512939	0.821142006	1.149385529	0.98	0.808086911****	0.808086910****	
	J5	0.561901817	0.92859014	0.381408975	0.96	0.500266896***	0.499507868***	
	J6	0.704707785	0.968231091	0.868430952	0.99	0.774819744*	0.773318788***	
	J9	0.57785045	0.958883109	0.428976229	0.95	0.273413816****	0.272546021****	
	J10	0.575876002	0.958942832	0.421644097	0.95	0.269008315****	0.268181011****	
	J11	0.519950542	0.921988184	0.319076866	0.94	0.115949395****	0.114751701****	
	J12	0.868601135	0.854974054	1.127761334	0.97	0.907475561**	0.907475561**	
	J13	0.519844649	0.923659949	0.335970003	0.94	0.118958992****	0.117727387****	
	J14	0.575876002	0.958942832	0.421644097	0.95	0.269008315****	0.268181011****	
	J16	0.561901817	0.92859014	0.381408975	0.96	0.500266896***	0.499507868***	
	Kobe	J1	0.912992596	0.886973614	0.892190258	0.83	0.716891908****	0.0326959975****
		J2	0.896803419	0.878782809	0.854764304	0.89	0.777254964****	0.721283015****
		J3	0.830124176	0.955150948	0.260896884	0.8	0.235031528****	0.235031528****
J4		1.162606767	0.931868392	1.904965796	1.12	0.97504195***	0.721283015****	
J5		0.825554172	0.957265011	0.26588304	0.8	0.226248887****	0.226248887****	
J6		0.896803419	0.878782809	0.854764304	0.89	0.777254964****	0.721283015****	
J9		0.969874553	0.913290297	0.525704815	0.73	0.50620424****	0.50620423****	
J10		0.961766278	0.905207925	0.516486981	0.73	0.500371149****	0.50037114****	
J11		0.961833619	0.942492242	0.277668003	0.64	0.130153553****	0.130153553****	
J12		0.987498387	0.914356633	1.191558868	1.02	0.981814257***	0.721283015****	
J13		0.959291488	0.940916791	0.279904107	0.64	0.119001377****	0.119001377****	
J14		0.961766278	0.905207925	0.516486981	0.73	0.500371149***	0.500371149****	
J16		0.825554172	0.957265011	0.26588304	0.8	0.226248887****	0.226248887****	

6. Conclusion

In this study, a new intelligent control model was developed and used for vibration reduction of the highway bridge, employing a single-agent Centralized Replicator Controller "CRC" and a decentralized Multi-Agent Replicator Controller "MARC". The controller incorporated with an improved version of the non-dominated sorting genetic algorithm known as NSGA-II. MR dampers are used as a semi-active control device to improve the isolation system. This research proved the high performance of optimal replicator dynamic controller for vibration reduction of the real structure. The importance of using an adaptive algorithm relates to the system's ability to deal with uncertainty. The design of the controller is novel. Since, this is the first time that an optimal replicator dynamic controller designed with the integration of RD with NSGA-II and has been used for vibration control in civil structures. The selection of the growth rate parameter is crucial to replicator dynamics. The values of the growth rate were determined by minimizing 13 objective functions. The objective functions in this study are maximum base shear (J1), overturning moment (J2), midspan displacement (J3), acceleration (J4), maximum bearing deformation (J5), maximum ductility (J6), maximum RMS of base shear (J9), maximum RMS of base moment (J10), maximum RMS of midspan displacement (J11), maximum RMS of midspan acceleration (J12), and maximum RMS of abutment displacement (J13).

7. Declarations

7.1. Author Contributions

Conceptualization, Z.M. and A.B.; methodology, Z.M.; software, Z.M.; validation, Z.M. and A.B.; formal analysis, Z.M.; investigation, Z.M.; resources, Z.M.; data curation, Z.M.; writing—original draft preparation, Z.M.; writing—review and editing, Z.M.; visualization, Z.M.; supervision, A.B.; project administration, Z.M.; funding acquisition, A.B. All authors have read and agreed to the published version of the manuscript.

7.2. Data Availability Statement

The data presented in this study are available on request from the corresponding author.

7.3. Funding

The authors received no financial support for the research, authorship, and/or publication of this article.

7.4. Conflicts of Interest

The authors declare no conflict of interest.

8. References

- [1] Agrawal, A., Tan, P., Nagarajaiah, S., & Zhang, J. (2009). Benchmark structural control problem for a seismically excited highway bridge-part I: Phase I problem definition. *Structural Control and Health Monitoring*, 16(5), 509–529. doi:10.1002/stc.301.
- [2] Tan, P., & Agrawal, A. K. (2009). Benchmark structural control problem for a seismically excited highway bridge-Part II: Phase I Sample control designs. *Structural Control and Health Monitoring*, 16(5), 530–548. doi:10.1002/stc.300.
- [3] Nagarajaiah, S., Narasimhan, S., Agrawal, A., & Tan, P. (2009). Benchmark structural control problem for a seismically excited highway bridge-part III: Phase II sample controller for the fully base-isolated case. *Structural Control and Health Monitoring*, 16(5), 549–563. doi:10.1002/stc.293.
- [4] Javadinasab Hormozabad, S., & Gutierrez Soto, M. (2021). Load balancing and neural dynamic model to optimize replicator dynamics controllers for vibration reduction of highway bridge structures. *Engineering Applications of Artificial Intelligence*, 99, 104138. doi:10.1016/j.engappai.2020.104138.
- [5] Camara, A. (2018). Seismic behavior of cable-stayed bridges: a review. *MOJ Civil Engineering*, 4(3), 161–169. doi:10.15406/mojce.2018.04.00115.
- [6] Dolce, M., Cardone, D., Ponzio, F. C., & Valente, C. (2005). Shaking table tests on reinforced concrete frames without and with passive control systems. *Earthquake Engineering and Structural Dynamics*, 34(14), 1687–1717. doi:10.1002/eqe.501.
- [7] Soong, T. T., & Constantinou, M. C. (Eds.). (2014). *Passive and active structural vibration control in civil engineering*. Springer, Vienna, Austria.
- [8] Chen, Z., Fang, H., Han, Z., & Sun, S. (2019). Influence of bridge-based designed TMD on running trains. *JVC/Journal of Vibration and Control*, 25(1), 182–193. doi:10.1177/1077546318773022.
- [9] Li, J., Zhang, H., Chen, S., & Zhu, D. (2020). Optimization and sensitivity of TMD parameters for mitigating bridge maximum vibration response under moving forces. *Structures*, 28, 512–520. doi:10.1016/j.istruc.2020.08.065.
- [10] Alizadeh, H., & Hosseni Lavassani, S. H. (2021). Flutter Control of Long Span Suspension Bridges in Time Domain Using Optimized TMD. *International Journal of Steel Structures*, 21(2), 731–742. doi:10.1007/s13296-021-00469-y.

- [11] Bharathi Priya C., & Gopalakrishnan, N. (2022). Emotional Learning based adaptive control algorithm for Semi-Active seismic control of structures. *Materials Today: Proceedings*, 65, 1703–1710. doi:10.1016/j.matpr.2022.04.714.
- [12] Kemerli, M., Şahin, Ö., Yazıcı, İ., Çağlar, N., & Engin, T. (2022). Comparison of discrete-time sliding mode control algorithms for seismic control of buildings with magnetorheological fluid dampers. *JVC/Journal of Vibration and Control*, 10775463211070062. doi:10.1177/10775463211070062.
- [13] Jian, L., Song, F., & Huang, Y. (2020). Research on Semiactive Control of Civil Engineering Structure Based on Neural Network. *Wireless Communications and Mobile Computing*, 2020. doi:10.1155/2020/8842031.
- [14] Javadinasab H., S., & Ghorbani-Tanha, A. K. (2020). Semi-active fuzzy control of Lali Cable-Stayed Bridge using MR dampers under seismic excitation. *Frontiers of Structural and Civil Engineering*, 14(3), 706–721. doi:10.1007/s11709-020-0612-9.
- [15] Bathaei, A., & Zahrai, S. M. (2022). Compensating time delay in semi-active control of a SDOF structure with MR damper using predictive control. *Structural Engineering and Mechanics*, 82(4), 445–458. doi:10.12989/sem.2022.82.4.445.
- [16] Saeed, M. U., Sun, Z., & Elias, S. (2022). Research developments in adaptive intelligent vibration control of smart civil structures. *Journal of Low Frequency Noise Vibration and Active Control*, 41(1), 292–329. doi:10.1177/14613484211032758.
- [17] Fisco, N. R., & Adeli, H. (2011). Smart structures: Part II - Hybrid control systems and control strategies. *Scientia Iranica*, 18(3 A), 285–295. doi:10.1016/j.scient.2011.05.035.
- [18] Alkhatib, R., & Golnaraghi, M. F. (2003). Active structural vibration control: A review. *Shock and Vibration Digest*, 35(5), 367–383. doi:10.1177/05831024030355002.
- [19] Gutierrez Soto, M., & Adeli, H. (2017). Recent advances in control algorithms for smart structures and machines. *Expert Systems*, 34(2), 12205. doi:10.1111/exsy.12205.
- [20] Gutierrez Soto, M. (2018). Bio-inspired hybrid vibration control methodology for intelligent isolated bridge structures. *Active and Passive Smart Structures and Integrated Systems XII*. doi:10.1117/12.2300393.
- [21] Gutierrez Soto, M., & Adeli, H. (2018). Vibration control of smart base-isolated irregular buildings using neural dynamic optimization model and replicator dynamics. *Engineering Structures*, 156, 322–336. doi:10.1016/j.engstruct.2017.09.037.
- [22] Gutierrez Soto, M., & Adeli, H. (2017). Many-objective control optimization of high-rise building structures using replicator dynamics and neural dynamics model. *Structural and Multidisciplinary Optimization*, 56(6), 1521–1537. doi:10.1007/s00158-017-1835-9.
- [23] Soto, G., & Adeli, H. (2017). Multi-agent replicator controller for sustainable vibration control of smart structures mariantonieta. *Journal of Vibroengineering*, 19(6), 4300–4322. doi:10.21595/jve.2017.18924.
- [24] Gutierrez Soto, M. (2017). Multi-agent Replicator Control Methodologies for Sustainable Vibration Control of Smart Building and Bridge Structures. Ph.D. Thesis, Ohio State University, Columbus, United States.
- [25] Gutierrez Soto, M., & Adeli, H. (2019). Semi-active vibration control of smart isolated highway bridge structures using replicator dynamics. *Engineering Structures*, 186, 536–552. doi:10.1016/j.engstruct.2019.02.031.
- [26] Ramezani, M., Bathaei, A., & Zahrai, S. M. (2019). Comparing fuzzy type-1 and -2 in semi-active control with TMD considering uncertainties. *Smart Structures and Systems*, 23(2), 155–171. doi:10.12989/sss.2019.23.2.155.
- [27] Bathaei, A., & Zahrai, S. M. (2022). Improving semi-active vibration control of an 11-story structure with non-linear behavior and floating fuzzy logic algorithm. *Structures*, 39, 132–146. doi:10.1016/j.istruc.2022.03.022.
- [28] Cui, Y., Geng, Z., Zhu, Q., & Han, Y. (2017). Review: Multi-objective optimization methods and application in energy saving. *Energy*, 125, 681–704. doi:10.1016/j.energy.2017.02.174.
- [29] Branke, J., Kaußler, T., & Schmeck, H. (2001). Guidance in evolutionary multi-objective optimization. *Advances in Engineering Software*, 32(6), 499–507. doi:10.1016/S0965-9978(00)00110-1.
- [30] Deb, K. (1999). Evolutionary algorithms for multi-criterion optimization in engineering design. *Evolutionary algorithms in engineering and computer science*, 2, 135-161.
- [31] Srinivas, N., & Deb, K. (1994). Multiobjective Optimization Using Nondominated Sorting in Genetic Algorithms. *Evolutionary Computation*, 2(3), 221–248. doi:10.1162/evco.1994.2.3.221.
- [32] Deb, K., Pratap, A., Agarwal, S., & Meyarivan, T. (2002). A fast and elitist multi-objective genetic algorithm: NSGA-II. *IEEE Transactions on Evolutionary Computation*, 6(2), 182–197. doi:10.1109/4235.996017.
- [33] Quijano, N., Ocampo-Martinez, C., Barreiro-Gomez, J., Obando, G., Pantoja, A., & Mojica-Nava, E. (2017). The role of population games and evolutionary dynamics in distributed control systems: The advantages of evolutionary game theory. *IEEE Control Systems*, 37(1), 70–97. doi:10.1109/MCS.2016.2621479.

- [34] Song, G., Sethi, V., & Li, H. N. (2006). Vibration control of civil structures using piezoceramic smart materials: A review. *Engineering Structures*, 28(11), 1513-1524. doi:10.1016/j.engstruct.2006.02.002.
- [35] Gunantara, N. (2018). A review of multi-objective optimization: Methods and its applications. *Cogent Engineering*, 5(1), 1–16. doi:10.1080/23311916.2018.1502242.
- [36] Yusoff, Y., Ngadiman, M. S., & Zain, A. M. (2011). Overview of NSGA-II for Optimizing Machining Process Parameters. *Procedia Engineering*, 15, 3978–3983. doi:10.1016/j.proeng.2011.08.745.
- [37] Makris, N., & Zhang, J. (2004). Seismic response analysis of a highway overcrossing equipped with elastomeric bearings and fluid dampers. *Journal of Structural Engineering*, 130(6), 830-845. doi:10.1061/(asce)0733-9445(2004)130:6(830).